

Electronic Supplementary Information

Luminescent iridium(III) 2-cyanobenzothiazole complexes as site-specific labels to afford peptide-based phosphorogenic probes and hydrogels for enzyme activity sensing, cancer imaging and photodynamic therapy

Jun-Wen Xu,^a Lawrence Cho-Cheung Lee,^a Alex Man-Hei Yip,^{a,b} Guang-Xi Xu,^a Peter Kam-Keung Leung^{a,c} and Kenneth Kam-Wing Lo^{*a,c}

^a Department of Chemistry, City University of Hong Kong, Tat Chee Avenue, Kowloon, Hong Kong, P. R. China; Email: bhkenlo@cityu.edu.hk

^b Laboratory for Synthetic Chemistry and Chemical Biology Limited, Units 1503–1511, 15/F, Building 17 W, Hong Kong Science Park, New Territories, Hong Kong, P. R. China

^c State Key Laboratory of Terahertz and Millimetre Waves, City University of Hong Kong, Tat Chee Avenue, Kowloon, Hong Kong, P. R. China

Table of Contents

Table S1	Electronic absorption spectral data of complexes 1 – 3 at 298 K.	S6
Table S2	Singlet oxygen ($^1\text{O}_2$) generation quantum yields (Φ_Δ) of complexes 1 – 3 and conjugates 2-MMP and 2-MMP-QSY7 in aerated CH_3CN at 298 K.	S7
Table S3	Photophysical data of conjugates 2-MMP , 2-MMP-QSY7 and 2-VPMS at 298 K.	S8
Table S4	Förster resonance energy transfer (FRET) parameters of conjugate 2-MMP-QSY7 .	S9
Table S5	(Photo)cytotoxicity (IC_{50}) of conjugate 2-MMP-QSY7 towards MDA-MB-231 and HEK-293 cells. Photocytotoxicity index (PI) = $\text{IC}_{50,\text{drak}}/\text{IC}_{50,\text{light}}$.	S10
Table S6	Cellular uptake of conjugate 2-MMP-QSY7 .	S11
Fig. S1	Electronic absorption spectra of complexes 1 – 3 in CH_2Cl_2 (black) and CH_3CN (red) at 298 K.	S12
Fig. S2	Normalised emission spectra of complexes 1 – 3 in degassed CH_2Cl_2 (black) and CH_3CN (red) at 298 K and in alcohol glass at 77 K (blue) ($\lambda_{\text{ex}} = 350 \text{ nm}$).	S13
Fig. S3	HPLC chromatograms ($\lambda_{\text{abs}} = 350 \text{ nm}$) of complexes 1 – 3 (100 μM) (black) and the reaction mixtures of complexes 1 – 3 (100 μM) and L-cysteine (L-Cys) (250 μM) in phosphate-buffered saline (PBS) (pH	S14

7.4)/CH₃CN (9:1, v/v) containing tris(2-carboxyethyl) phosphine (TCEP) (100 μM) after incubation at 298 K for 4 h (red).

- Fig. S4** ESI mass spectra of the eluent collected at $t_R = 20.2$ min (**1-Cys**), 18.2 min (**2-Cys**) and 20.9 min (**3-Cys**). S15
- Fig. S5** ESI mass spectra of a mixture of complex **2** (100 μM) and glutathione (250 μM), histidine (250 μM), lysine (250 μM), serine (250 μM), or threonine (250 μM) in PBS (pH 7.4)/CH₃CN (9:1, v/v) after incubation at 37°C for 12 h. S16
- Fig. S6** HPLC chromatograms ($\lambda_{abs} = 350$ nm) of conjugates **2-MMP** ($t_R = 15.56$ min), **2-MMP-QSY7** ($t_R = 15.83$ min) and **2-VPMS** ($t_R = 14.12$ min). S17
- Fig. S7** ESI mass spectra of purified conjugates **2-MMP**, **2-MMP-QSY7** and **2-VPMS** in CH₃OH at 298 K. S18
- Fig. S8** Spectral overlap of the absorption spectrum of the acceptor QSY-7 (black) and normalised emission spectrum of the donor conjugate **2-MMP** (red) in H₂O/CH₃CN (1:1, v/v) at 298 K. S19
- Fig. S9** HPLC chromatograms ($\lambda_{abs} = 350$ and 560 nm) of (a) conjugate **2-MMP-QSY7** (5 μM) before (black) and after (red) incubation with matrix metalloproteinase (MMP)-2 (0.002 mg mL⁻¹ in PBS) in aerated MMP reaction buffer/DMSO (99:1, v/v) at 37°C for 12 h. ESI mass spectra of cleavage products (b) **2-CVPMS** and (c) MRGGK-QSY7. S20
- Fig. S10** (a) SEM image and (b) EDS images and spectrum of **Gel-1**. Scale bar = 100 μm. S21

Fig. S11	Photographs of (a) Gel-1 ([Ir] = 80 μ M, 100 μ L) and (b) Gel-2 ([Ir] = 40 μ M, 100 μ L) upon addition of Dulbecco's Modified Eagle Medium (DMEM) (150 μ L) and incubation for 24, 48 and 72 h.	S22
Fig. S12	Optical microscopy images of MDA-MB-231 cells encapsulated by Gel-1 ([Ir] = 40 μ M, 100 μ L) at different focal lengths.	S23
Fig. S13	Analysis of live/dead MDA-MB-231 and HEK-293 cells using Calcein-AM (1 μ M, 30 min; λ_{ex} = 488 nm, λ_{em} = 510 – 540 nm) and propidium iodide (PI) (3 μ M, 30 min; λ_{ex} = 532 nm, λ_{em} = 610 – 640 nm). The cells were encapsulated by Gel-1 ([Ir] = 40 μ M) for 72 h. Scale bar = 100 μ m.	S24
Fig. S14	Laser-scanning confocal microscopy (LSCM) images of MDA-MB-231 cells encapsulated by Gel-1 ([Ir] = 40 μ M; λ_{ex} = 405 nm, λ_{em} = 570 – 620 nm) at 0, 6 and 18 h at 37°C. Scale bar = 20 μ m.	S25
Fig. S15	(a) SEM image and (b) EDS images and spectrum of Gel-2 . Scale bar = 100 μ m.	S26
Fig. S16	Intracellular reactive oxygen species (ROS) levels of Gel-2 ([Ir] = 80 μ M, 24 h)-pretreated MDA-MB-231 cells incubated with chloromethyl-2',7'-dichlorodihydrofluorescein diacetate (CM-H ₂ DCFDA) (10 μ M, 30 min; λ_{ex} = 488 nm, λ_{em} = 500 – 550 nm) without (left) or with (right) photoirradiation at 450 nm (15 mW cm ⁻²) for 30 min. Scale bar = 100 μ m.	S27
Fig. S17	¹ H NMR spectrum of the ligand bpy-CBT in (CD ₃) ₂ SO at 298 K.	S28
Fig. S18	¹ H NMR spectrum of complex 1 in (CD ₃) ₂ CO at 298 K.	S29

Fig. S19	^{13}C NMR spectrum of complex 1 in $(\text{CD}_3)_2\text{SO}$ at 298 K.	S30
Fig. S20	HR-ESI mass spectrum of complex 1 in CH_3OH at 298 K.	S31
Fig. S21	^1H NMR spectrum of complex 2 in $(\text{CD}_3)_2\text{CO}$ at 298 K.	S32
Fig. S22	^{13}C NMR spectrum of complex 2 in $(\text{CD}_3)_2\text{SO}$ at 298 K.	S33
Fig. S23	HR-ESI mass spectrum of complex 2 in CH_3OH at 298 K.	S34
Fig. S24	^1H NMR spectrum of complex 3 in $(\text{CD}_3)_2\text{CO}$ at 298 K.	S35
Fig. S25	^{13}C NMR spectrum of complex 3 in $(\text{CD}_3)_2\text{SO}$ at 298 K.	S36
Fig. S26	HR-ESI mass spectrum of complex 3 in CH_3OH at 298 K.	S37
Reference		S38

Table S1 Electronic absorption spectral data of complexes **1** – **3** at 298 K.

Complex	Solvent	$\lambda_{\text{abs}}/\text{nm}$ ($\epsilon/\text{dm}^3 \text{ mol}^{-1} \text{ cm}^{-1}$)
1	CH ₂ Cl ₂	256 sh (48,300), 309 (43,000), 364 sh (7,550)
	CH ₃ CN	259 sh (37,130), 308 (27,000), 360 sh (4,590)
2	CH ₂ Cl ₂	258 (67,070), 308 (46,005), 385 sh (7,655), 417 sh (3,560)
	CH ₃ CN	257 (63,425), 309 (42,925), 379 sh (7,355), 414 sh (3,750)
3	CH ₂ Cl ₂	261 (59,325), 293 (63,290), 349 (28,125), 370 sh (27,490), 472 sh (4,920)
	CH ₃ CN	261 (53,550), 291 (53,110), 346 (25,075), 366 sh (23,275), 475 sh (3,920)

Table S2 Singlet oxygen ($^1\text{O}_2$) generation quantum yields (Φ_Δ) of complexes **1** – **3** and conjugates **2-MMP** and **2-MMP-QSY7** in aerated CH_3CN at 298 K.

Complex/Conjugate	Φ_Δ^a
1	0.85
2	0.59
3	0.66
2-MMP	0.52
2-MMP-QSY7	0.06

^a $[\text{Ru}(\text{bpy})_3]\text{Cl}_2$ was used ($\Phi_\Delta = 0.57$ in aerated CH_3CN , $\lambda_{\text{ex}} = 450$ nm).

Table S3 Photophysical data of conjugates **2-MMP**, **2-MMP-QSY7** and **2-VPMS** at 298 K.

Conjugate	Solvent	λ_{em}/nm^a	$\tau_0/\mu s^b$	Φ_{em}^c
2-MMP	H ₂ O/CH ₃ CN ^d	608	0.15	0.07
2-MMP-QSY7	H ₂ O/CH ₃ CN ^d	623	0.13	< 0.005
2-VPMS	H ₂ O/CH ₃ CN ^d	590	0.19	0.08

^a $\lambda_{ex} = 350$ nm.

^b The lifetimes were measured at the emission maxima ($\lambda_{ex} = 355$ nm).

^c The emission quantum yields were determined using [Ru(bpy)₃]Cl₂ ($\Phi_{em} = 0.04$ in aerated H₂O, $\lambda_{ex} = 455$ nm) as a reference.¹

^d H₂O/CH₃CN (1:1, v/v).

Table S4 Förster resonance energy transfer (FRET) parameters of conjugate **2-MMP-QSY7**.

Donor	Acceptor	$J(\lambda)/\text{nm}^4 \text{ M}^{-1} \text{ cm}^{-1a}$	$R_0/\text{Å}$	$D/\text{Å}^b$	E_{calc}	E_{expt}
2-MMP	QSY-7	3.20×10^{15}	40.0	12.9	0.99	0.93

^a Overlap integral of the emission spectrum of the QSY-7-free conjugate **2-MMP** and the absorption spectrum of QSY-7 (acceptor).

^b Distance between the iridium(III) metal centre and centroid of QSY-7 in conjugate **2-MMP-QSY7**.

Table S5 (Photo)cytotoxicity (IC_{50}) of conjugate **2-MMP-QSY7** towards MDA-MB-231 and HEK-293 cells. Photocytotoxicity index (PI) = $IC_{50,drak}/IC_{50,light}$.

Cell line	$IC_{50,drak}/\mu M$	$IC_{50,light}/\mu M$	PI
MDA-MB-231	> 40	1.93 ± 0.18	> 20.7
HEK-293	> 40	10.17 ± 0.86	> 3.9

Table S6 Cellular uptake of conjugate **2-MMP-QSY7**.

Conjugate	Amount of iridium per cell/fmol ^a	
	MDA-MB-231	HEK-293
2-MMP-QSY7	0.38 ± 0.03	0.03 ± 0.004

^a Amount of iridium associated with an average MDA-MB-231 or HEK-293 cell upon incubation with the conjugate (10 μM) at 37°C for 4 h, as determined by ICP-MS.

Fig. S1 Electronic absorption spectra of complexes **1** – **3** in CH₂Cl₂ (black) and CH₃CN (red) at 298 K.

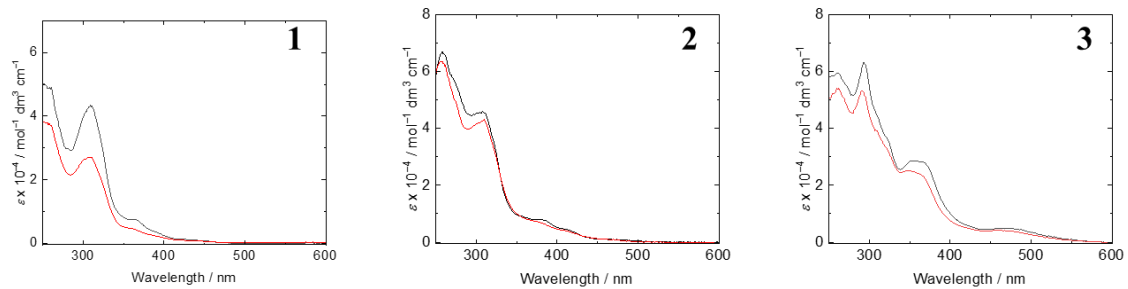


Fig. S2 Normalised emission spectra of complexes **1** – **3** in degassed CH_2Cl_2 (black) and CH_3CN (red) at 298 K and in alcohol glass at 77 K (blue) ($\lambda_{\text{ex}} = 350$ nm).

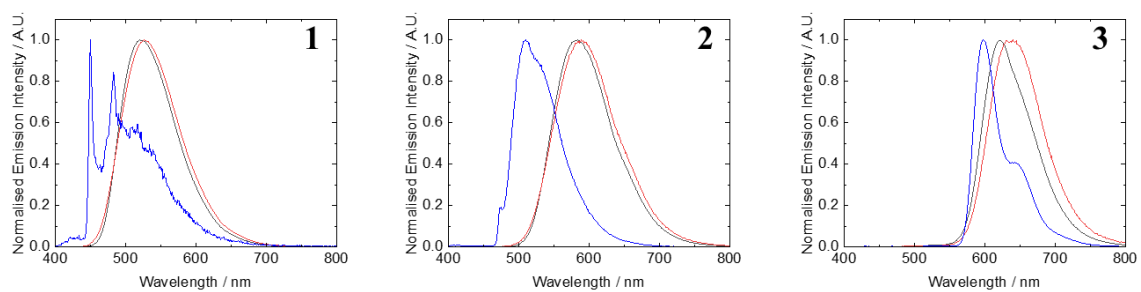


Fig. S3 HPLC chromatograms ($\lambda_{\text{abs}} = 350 \text{ nm}$) of complexes **1** – **3** (100 μM) (black) and the reaction mixtures of complexes **1** – **3** (100 μM) and L-cysteine (L-Cys) (250 μM) in phosphate-buffered saline (PBS) (pH 7.4)/CH₃CN (9:1, v/v) containing tris(2-carboxyethyl) phosphine (TCEP) (100 μM) after incubation at 298 K for 4 h (red).

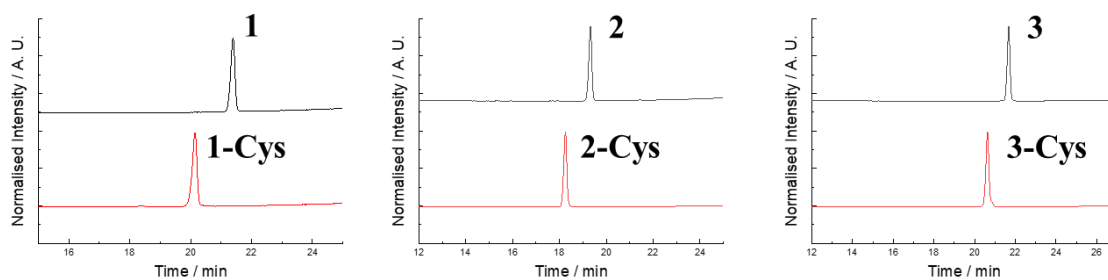


Fig. S4 ESI mass spectra of the eluent collected at $t_R = 20.2$ min (**1-Cys**), 18.2 min (**2-Cys**) and 20.9 min (**3-Cys**).

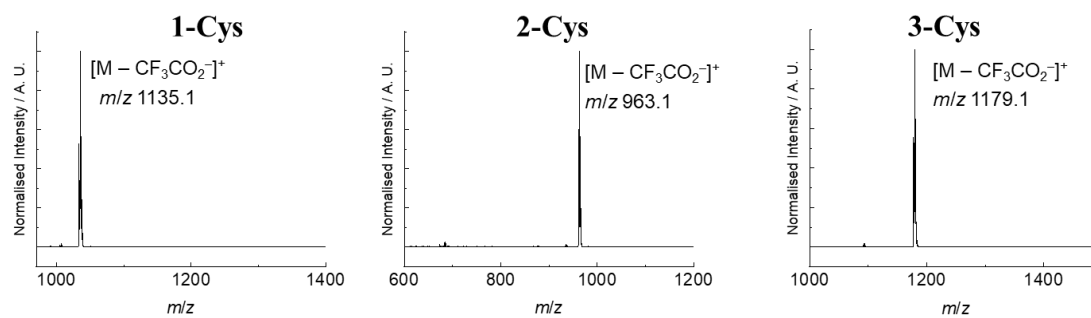


Fig. S5 ESI mass spectra of a mixture of complex **2** (100 μM) and glutathione (250 μM), histidine (250 μM), lysine (250 μM), serine (250 μM), or threonine (250 μM) in PBS (pH 7.4)/CH₃CN (9:1, v/v) after incubation at 37°C for 12 h.

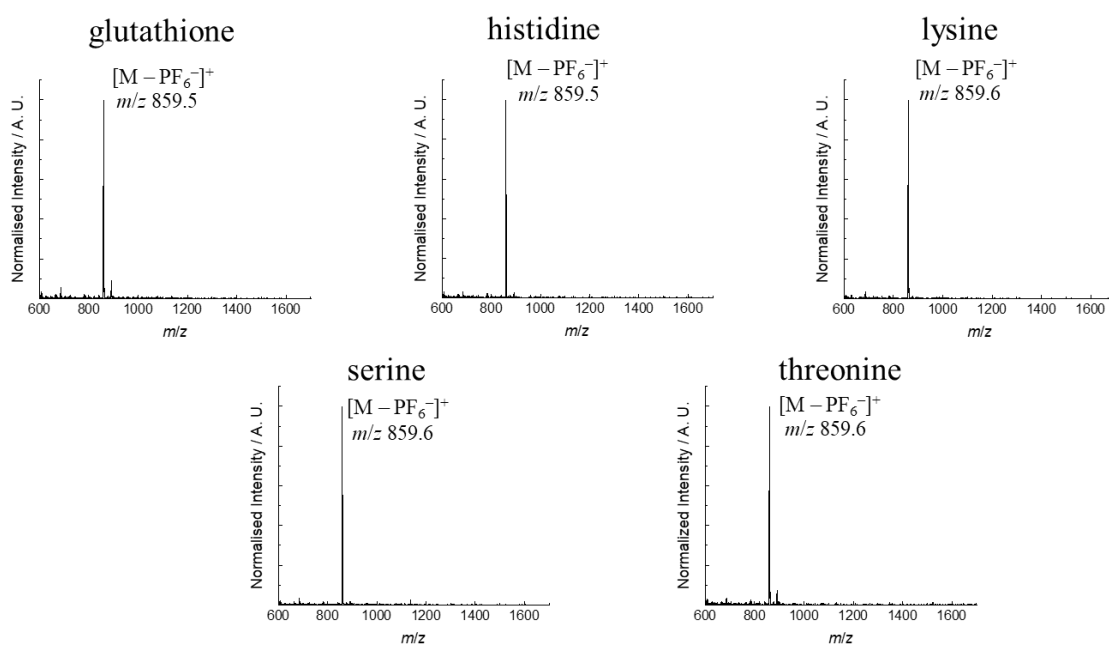


Fig. S6 HPLC chromatograms ($\lambda_{\text{abs}} = 350 \text{ nm}$) of conjugates **2-MMP** ($t_{\text{R}} = 15.56 \text{ min}$), **2-MMP-QSY7** ($t_{\text{R}} = 15.83 \text{ min}$) and **2-VPMS** ($t_{\text{R}} = 14.12 \text{ min}$).

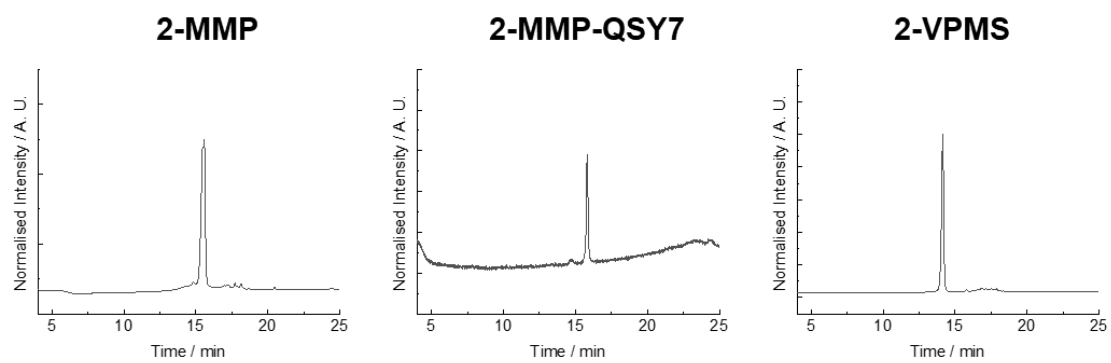


Fig. S7 ESI mass spectra of purified conjugates **2-MMP**, **2-MMP-QSY7** and **2-VPMS** in CH₃OH at 298 K.

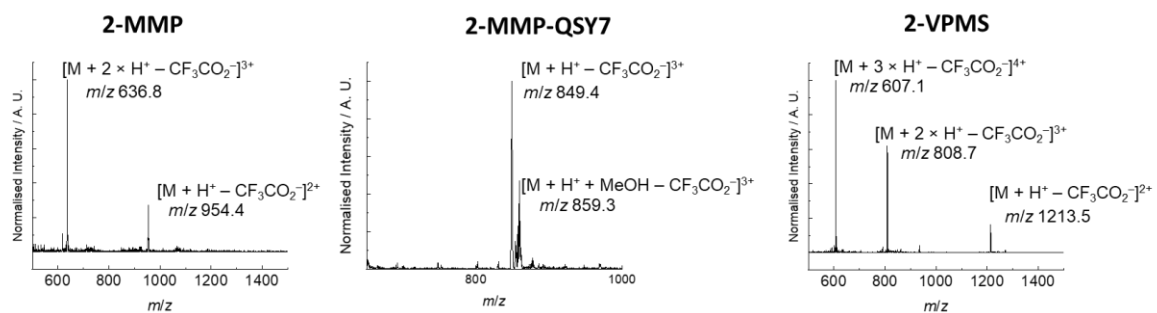


Fig. S8 Spectral overlap of the absorption spectrum of the acceptor QSY-7 (black) and normalised emission spectrum of the donor conjugate **2-MMP** (red) in H₂O/CH₃CN (1:1, v/v) at 298 K.

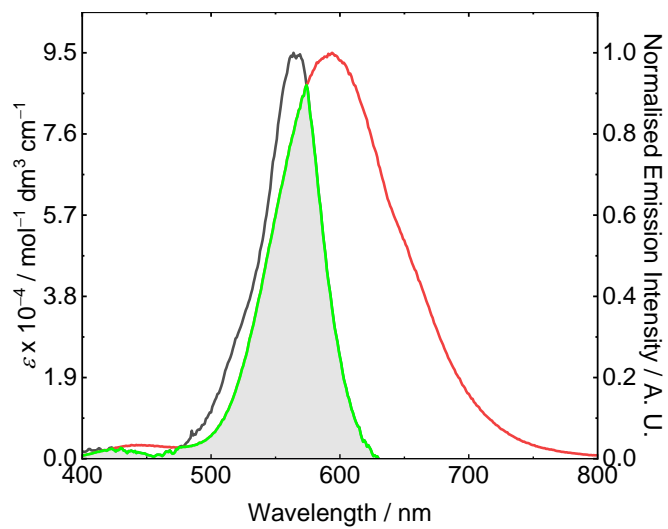


Fig. S9 HPLC chromatograms ($\lambda_{\text{abs}} = 350$ and 560 nm) of (a) conjugate **2-MMP-QSY7** ($5 \mu\text{M}$) before (black) and after (red) incubation with matrix metalloproteinase (MMP)-2 (0.002 mg mL^{-1} in PBS) in aerated MMP reaction buffer/DMSO ($99:1, v/v$) at 37°C for 12 h . ESI mass spectra of cleavage products (b) **2-CVPMS** and (c) MRGGK-QSY7.

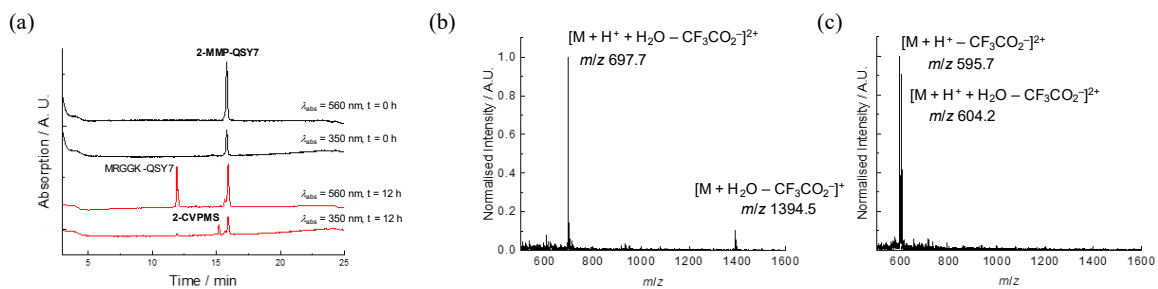


Fig. S10 (a) SEM image and (b) EDS images and spectrum of **Gel-1**. Scale bar = 100 μm .

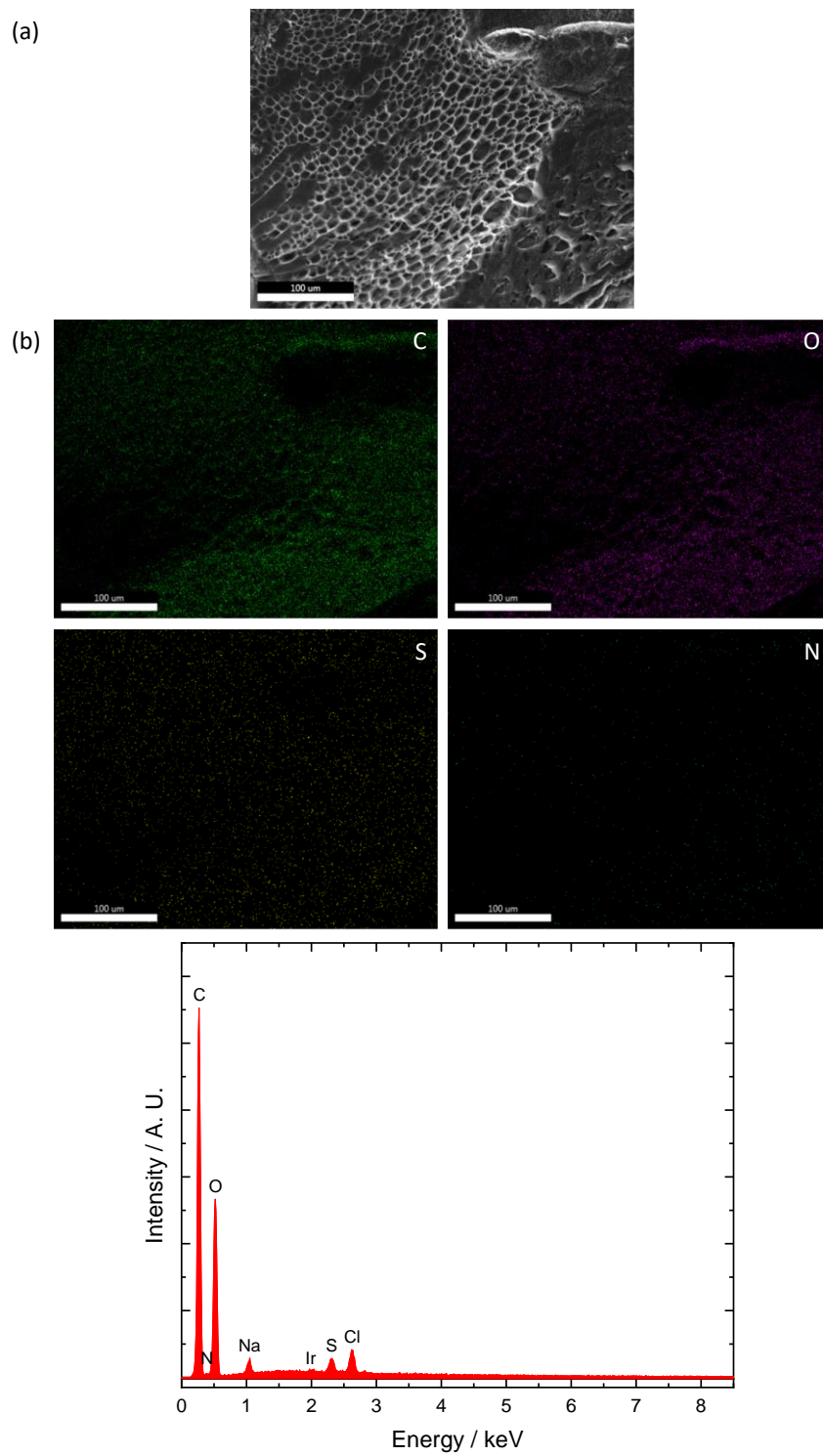


Fig. S11 Photographs of (a) **Gel-1** ($[Ir] = 80 \mu\text{M}$, $100 \mu\text{L}$) and (b) **Gel-2** ($[Ir] = 40 \mu\text{M}$, $100 \mu\text{L}$) upon addition of Dulbecco's Modified Eagle Medium (DMEM) ($150 \mu\text{L}$) and incubation for 24, 48 and 72 h.

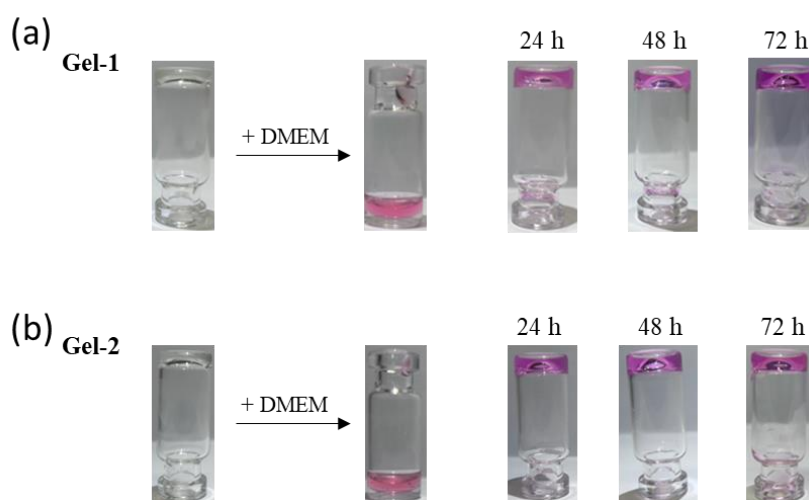


Fig. S12 Optical microscopy images of MDA-MB-231 cells encapsulated by **Gel-1** ($[Ir] = 40 \mu\text{M}$, $100 \mu\text{L}$) at different focal lengths.

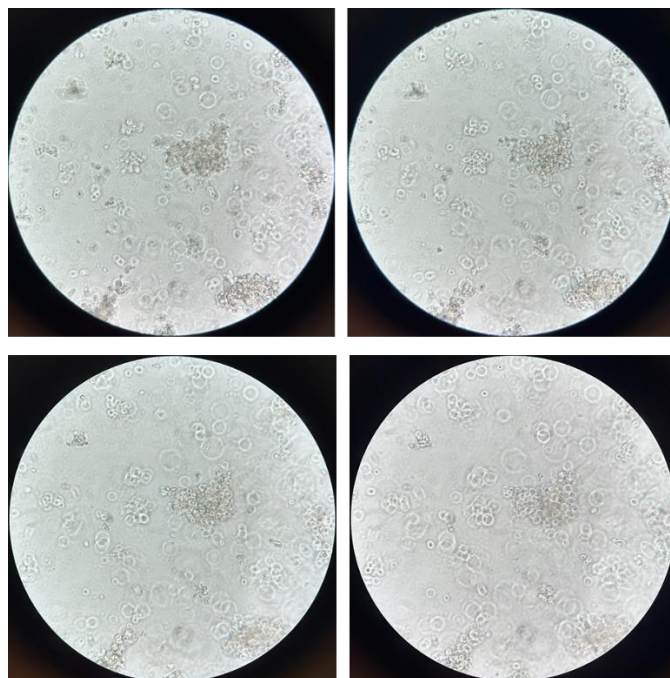


Fig. S13 Analysis of live/dead MDA-MB-231 and HEK-293 cells using Calcein-AM (1 μ M, 30 min; λ_{ex} = 488 nm, λ_{em} = 510 – 540 nm) and propidium iodide (PI) (3 μ M, 30 min; λ_{ex} = 532 nm, λ_{em} = 610 – 640 nm). The cells were encapsulated by **Gel-1** ([Ir] = 40 μ M) for 72 h. Scale bar = 100 μ m.

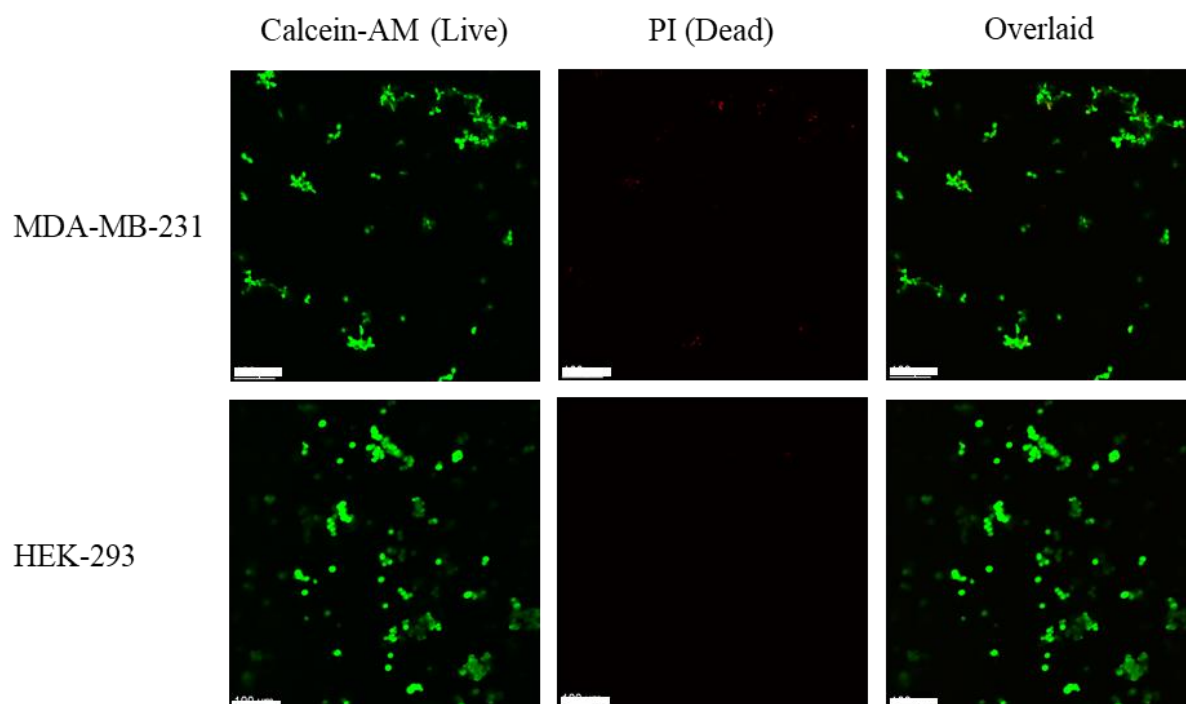


Fig. S14 Laser-scanning confocal microscopy (LSCM) images of MDA-MB-231 cells encapsulated by **Gel-1** ($[Ir] = 40 \mu\text{M}$; $\lambda_{\text{ex}} = 405 \text{ nm}$, $\lambda_{\text{em}} = 570 - 620 \text{ nm}$) at 0, 6 and 18 h at 37°C. Scale bar = 20 μm .

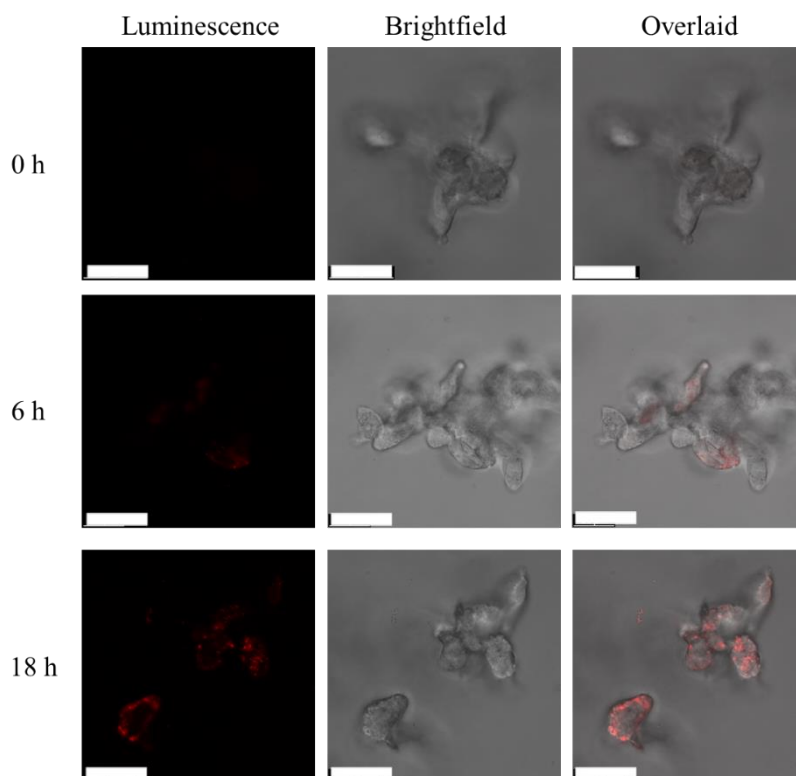


Fig. S15 (a) SEM image and (b) EDS images and spectrum of **Gel-2**. Scale bar = 100 μm .

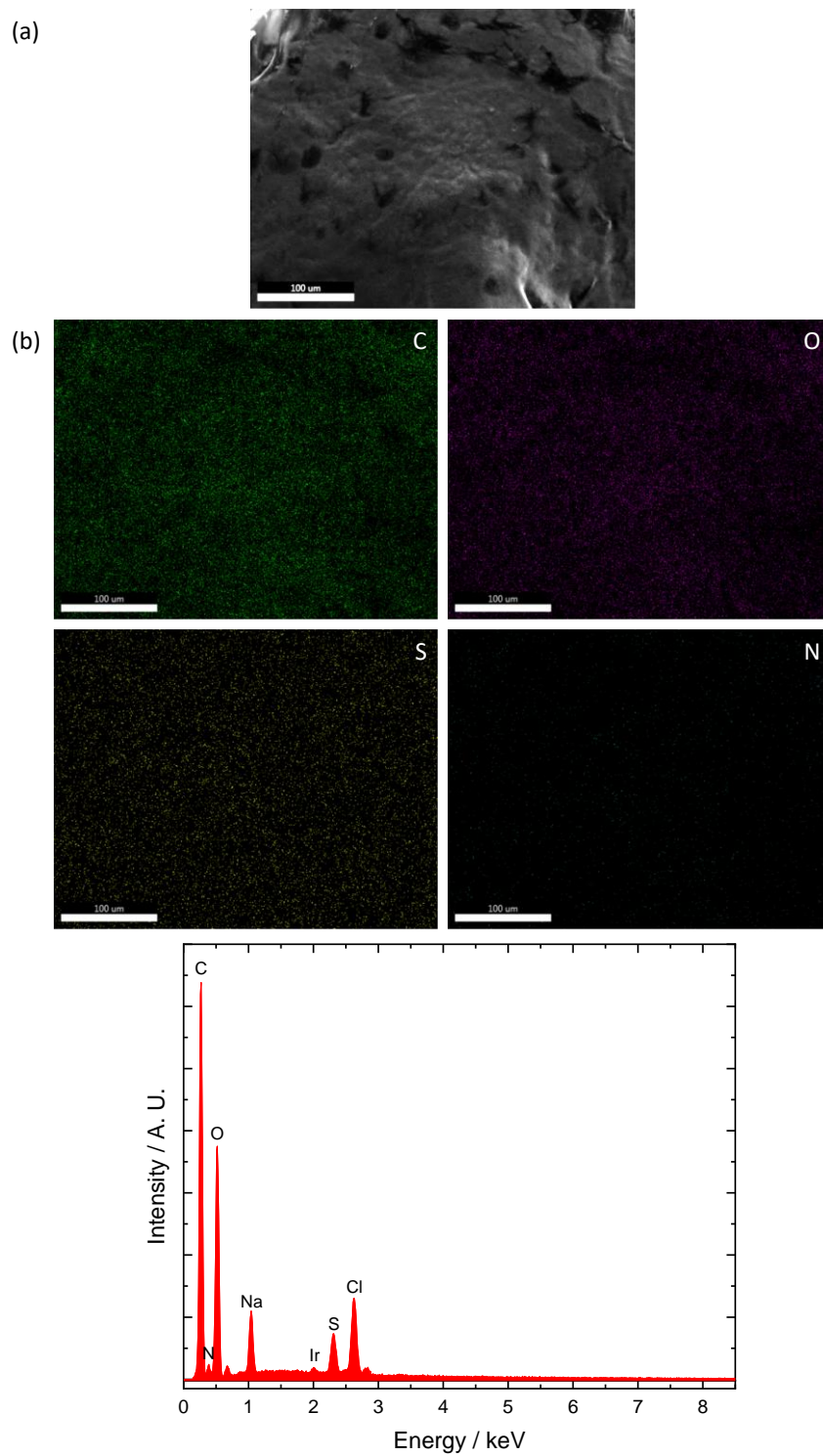


Fig. S16 Intracellular reactive oxygen species (ROS) levels of **Gel-2** ([Ir] = 80 μ M, 24 h)-pretreated MDA-MB-231 cells incubated with chloromethyl-2',7'-dichlorodihydrofluorescein diacetate (CM-H₂DCFDA) (10 μ M, 30 min; λ_{ex} = 488 nm, λ_{em} = 500 – 550 nm) without (left) or with (right) photoirradiation at 450 nm (15 mW cm⁻²) for 30 min. Scale bar = 100 μ m.

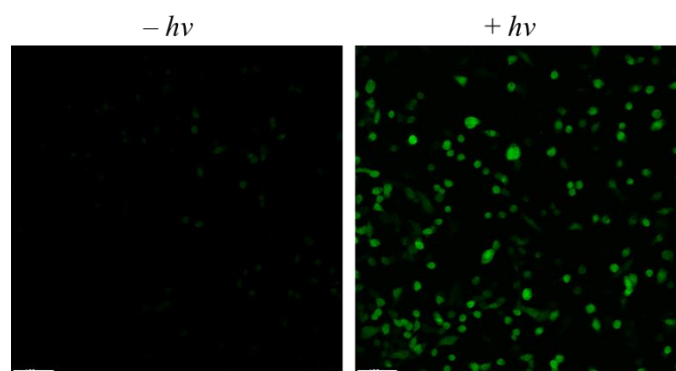


Fig. S17 ^1H NMR spectrum of the ligand bpy-CBT in $(\text{CD}_3)_2\text{SO}$ at 298 K.

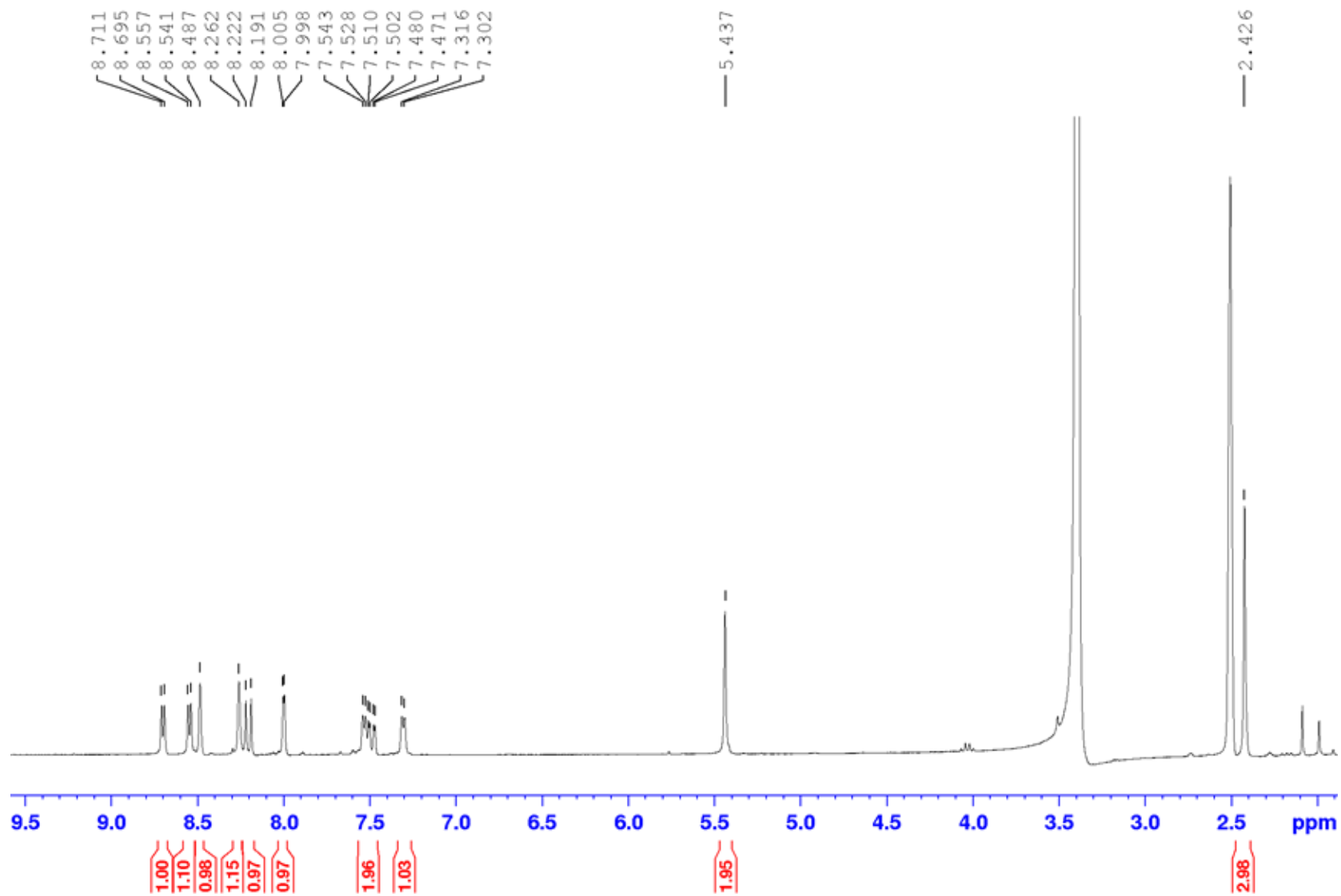


Fig. S18 ^1H NMR spectrum of complex 1 in $(\text{CD}_3)_2\text{CO}$ at 298 K.

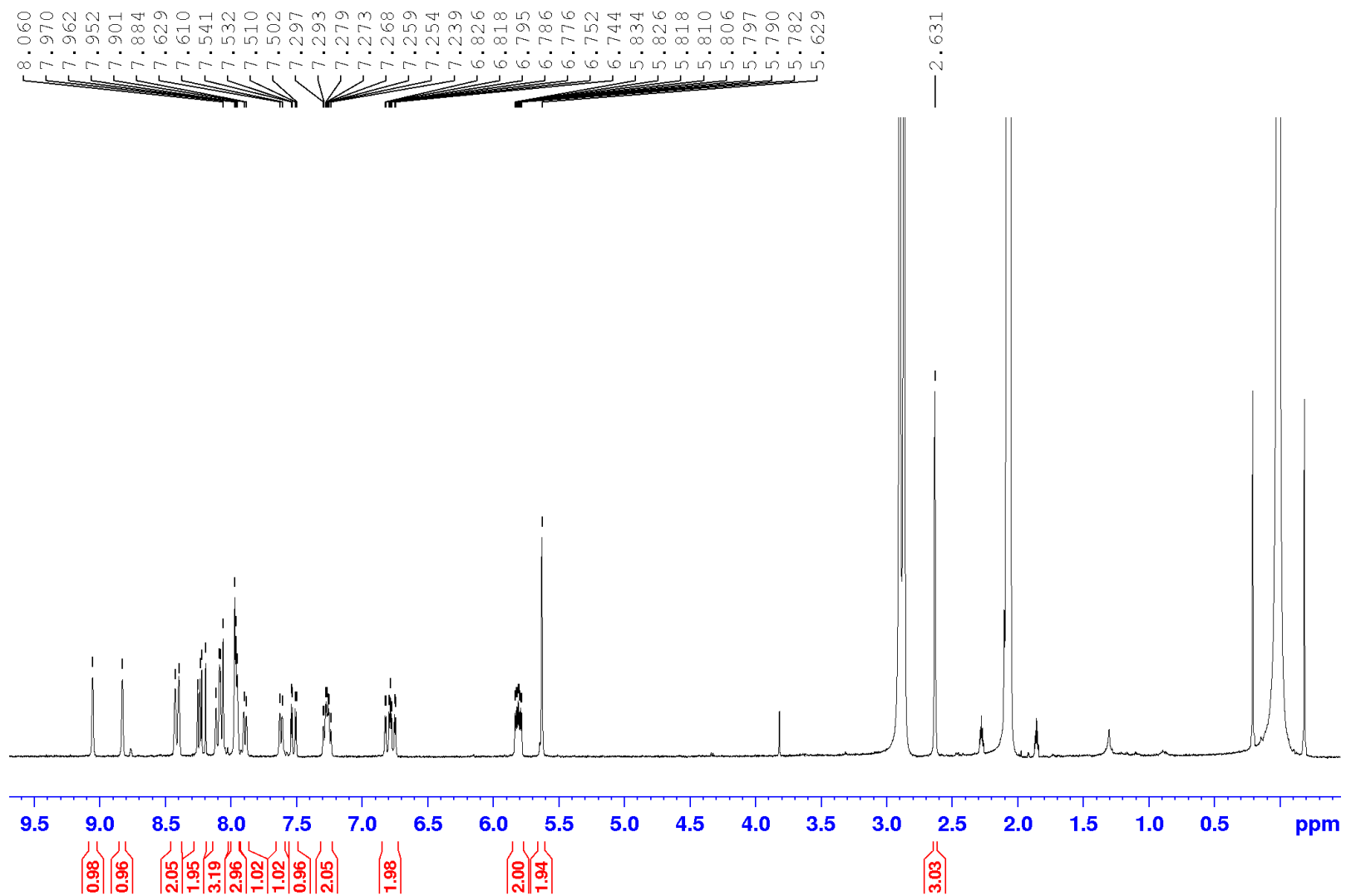


Fig. S19 ^{13}C NMR spectrum of complex **1** in $(\text{CD}_3)_2\text{SO}$ at 298 K.

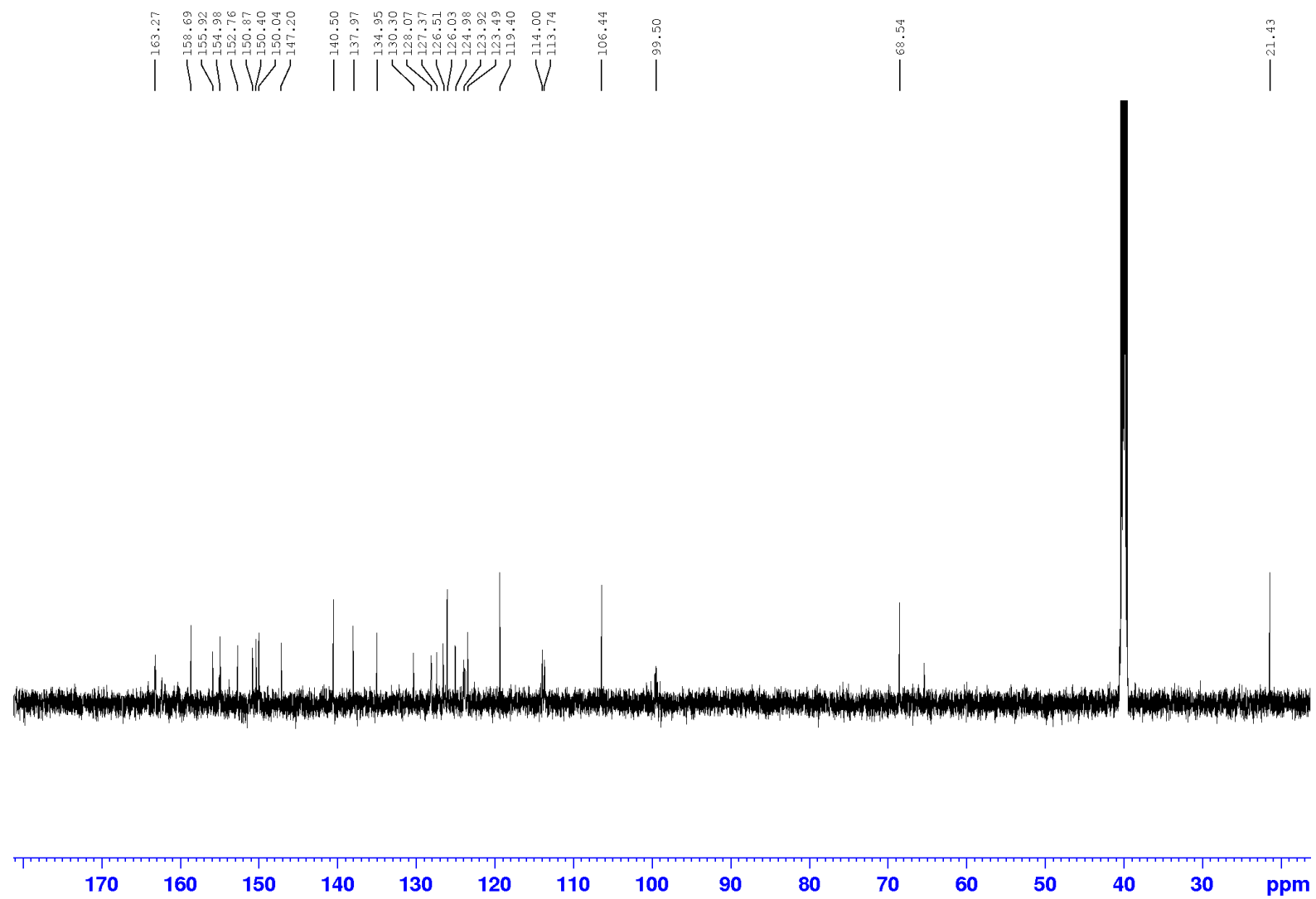


Fig. S20 HR-ESI mass spectrum of complex **1** in CH₃OH at 298 K.

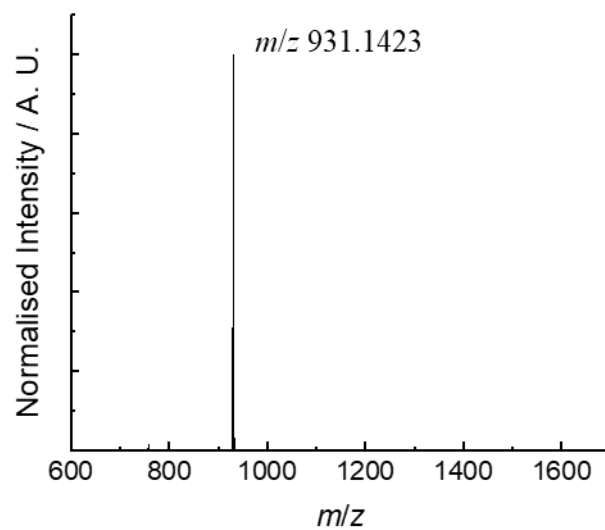


Fig. S21 ^1H NMR spectrum of complex **2** in $(\text{CD}_3)_2\text{CO}$ at 298 K.

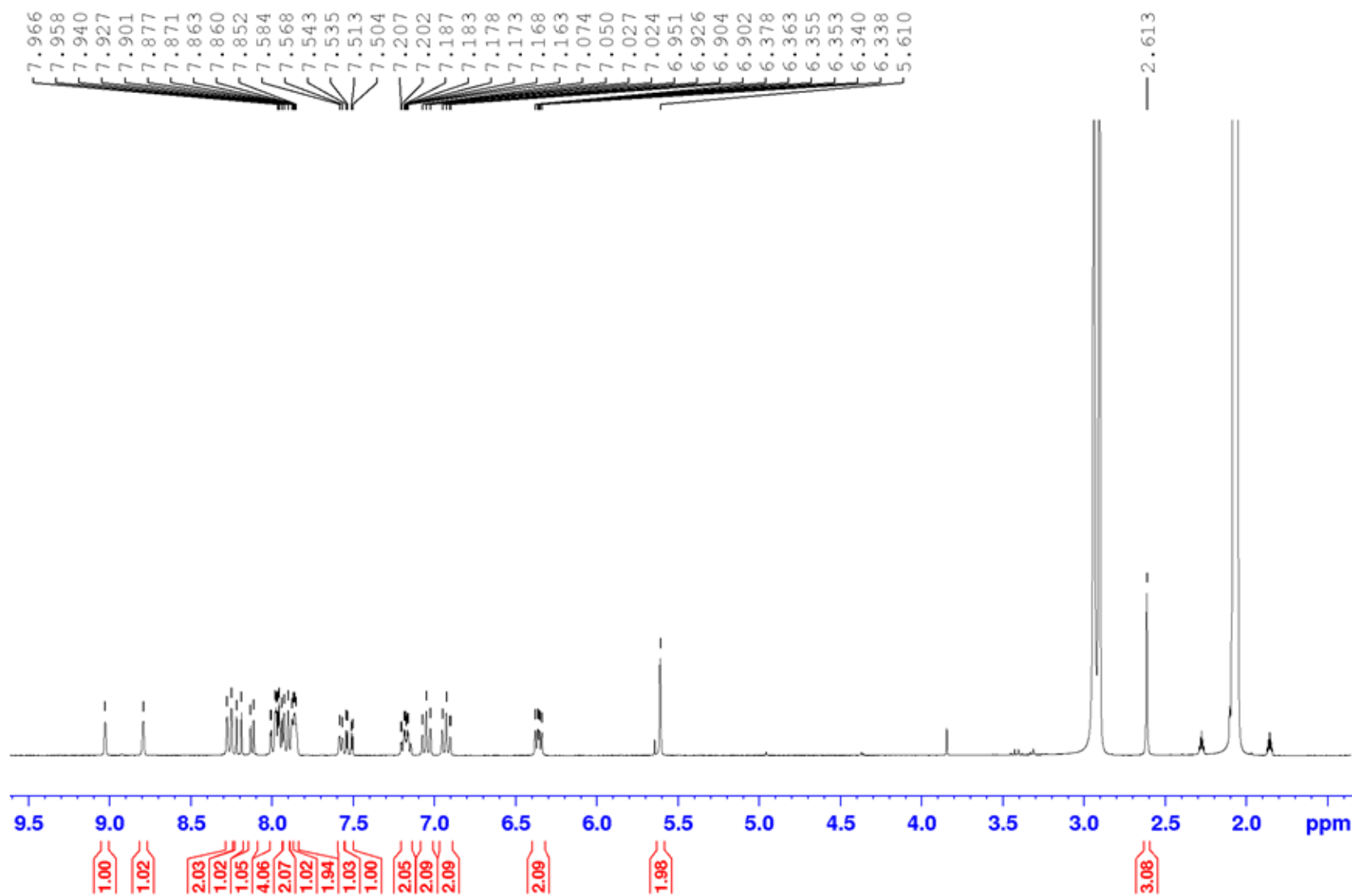


Fig. S22 ^{13}C NMR spectrum of complex **2** in $(\text{CD}_3)_2\text{SO}$ at 298 K.

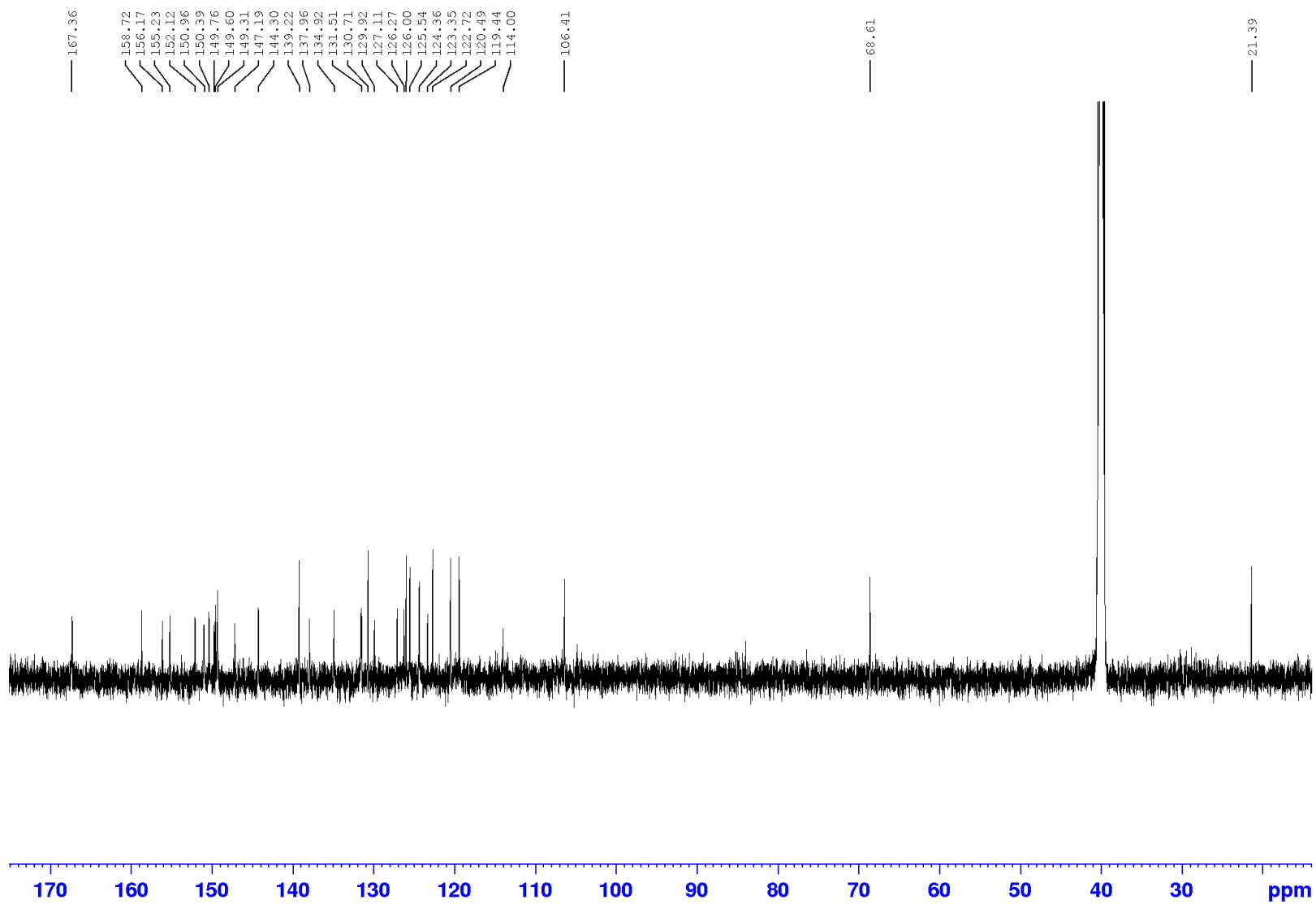


Fig. S23 HR-ESI mass spectrum of complex **2** in CH₃OH at 298 K.

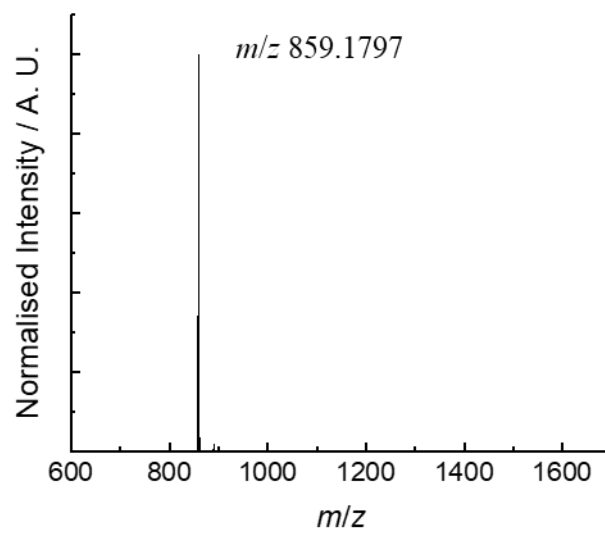


Fig. S24 ^1H NMR spectrum of complex **3** in $(\text{CD}_3)_2\text{CO}$ at 298 K.

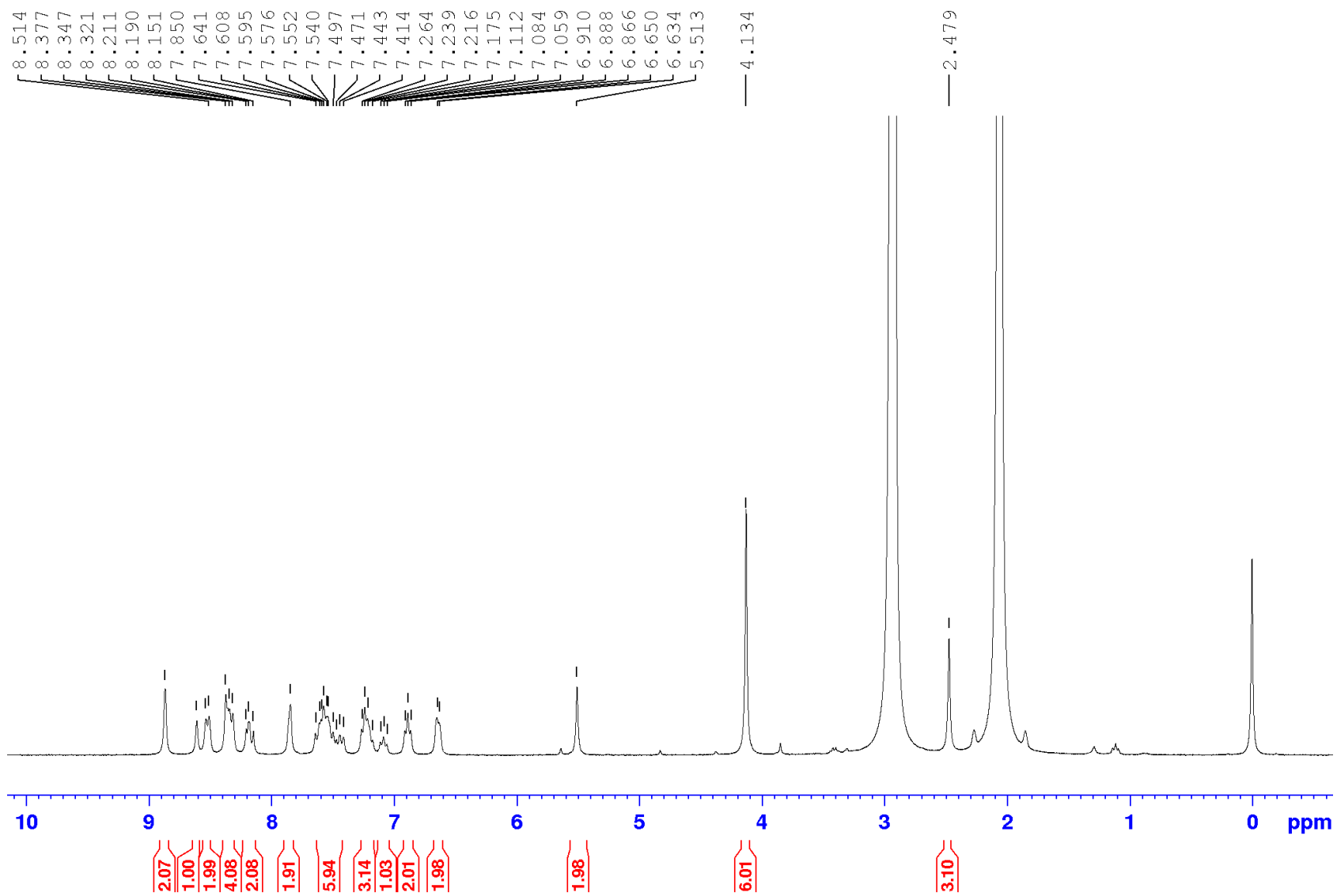


Fig. S25 ^{13}C NMR spectrum of complex **3** in $(\text{CD}_3)_2\text{SO}$ at 298 K.

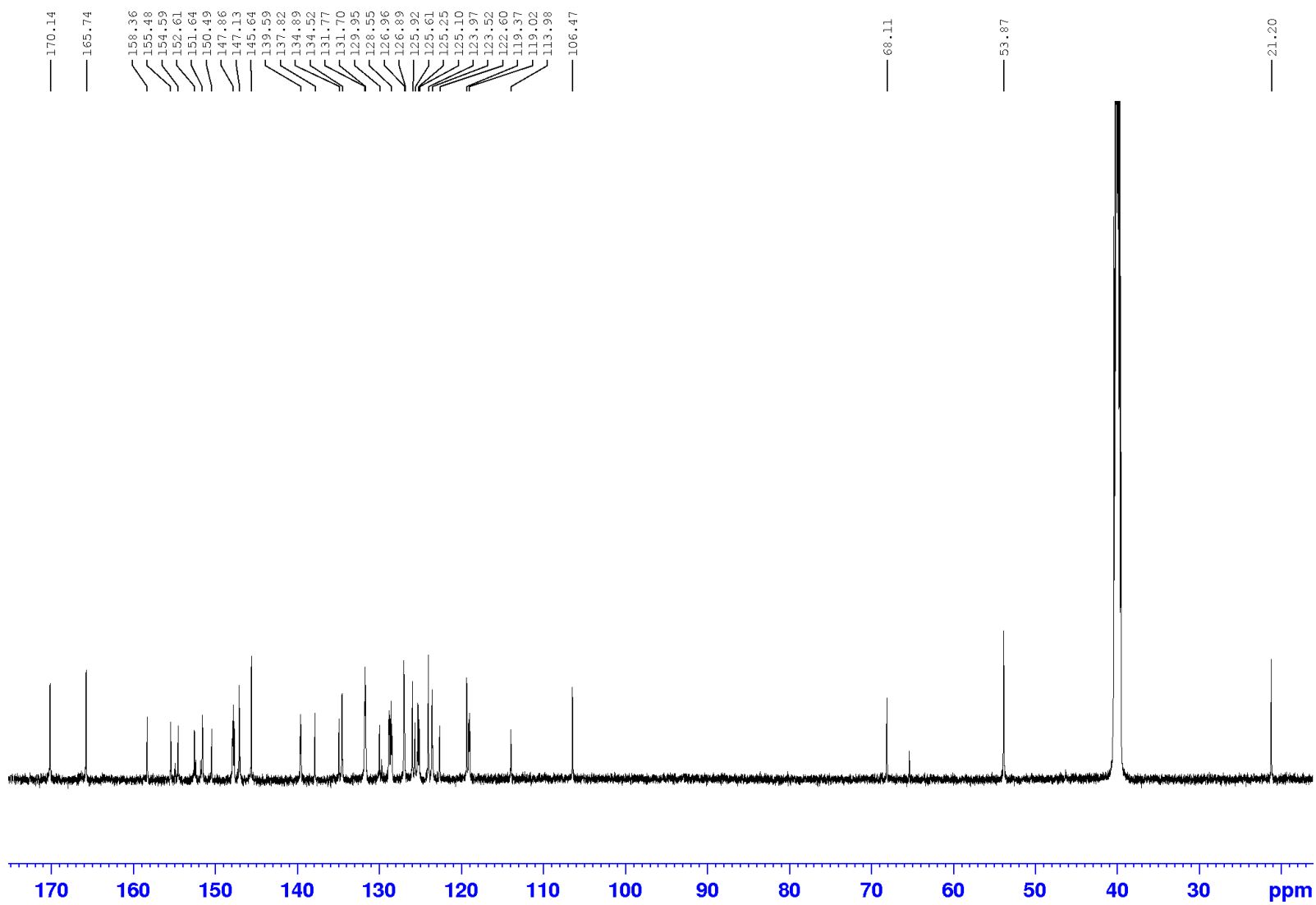
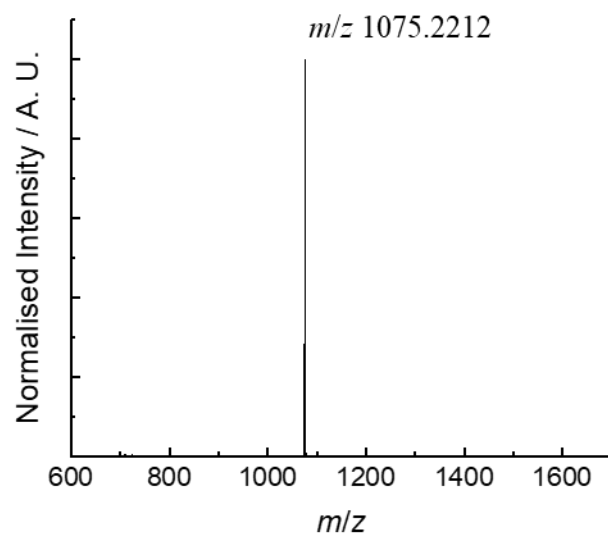


Fig. S26 HR-ESI mass spectrum of complex **3** in CH₃OH at 298 K.



Reference

1. K. Suzuki, A. Kobayashi, S. Kaneko, K. Takehira, T. Yoshihara, H. Ishida, Y. Shiina, S. Oishi and S. Tobita, *Phys. Chem. Chem. Phys.*, 2009, **11**, 9850–9860.